CHALMERS
UNIVERSITY OF TECHNOLOGY

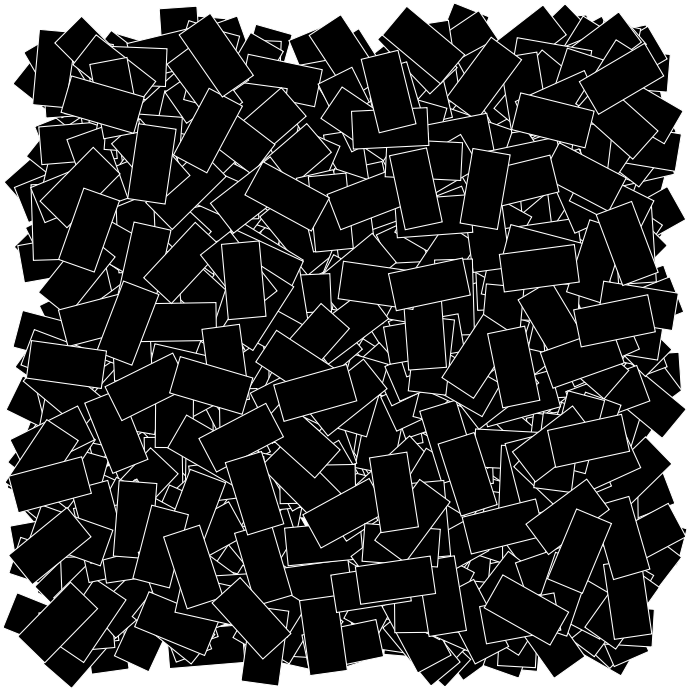

Manufacturing and Characterisation of Ultra-Stiff Composite Material

An Examination of Uniformly Oriented Ultra-Thin High Modulus CFRP Tape Composite Material

Master's thesis in Materials Engineering

MARCUS JOHANSEN

Department of Industrial and Materials Science
CHALMERS UNIVERSITY OF TECHNOLOGY
Gothenburg, Sweden 2019

Master's thesis 2019:06

Manufacturing and Characterisation of Ultra-Stiff Composite Material

An Examination of Uniformly Oriented Ultra-Thin High Modulus CFRP Tape Composite Material

MARCUS JOHANSEN

CHALMERS
UNIVERSITY OF TECHNOLOGY

Department of Industrial and Materials Science
Division of Material and Computational Mechanics
Chalmers University of Technology
Gothenburg, Sweden 2019

Manufacturing and Characterisation of Ultra-Stiff Composite Material
An Examination of Uniformly Oriented Ultra-Thin High Modulus CFRP Tape Composite Material
MARCUS JOHANSEN

Supervisor: Prof. Leif Asp, Department of Industrial and Materials Science
Examiner: Prof. Leif Asp, Department of Industrial and Materials Science

Master's Thesis 2019:06
Department of Industrial and Materials Science
Division of Material and Computational Mechanics
Chalmers University of Technology
SE-412 96 Gothenburg
Telephone +46 31 772 1000

Cover: An illustration of one thousand randomly oriented ultra-thin high modulus CFRP tapes.

Typeset in LaTeX
Gothenburg, Sweden 2019

Manufacturing and Characterisation of Ultra-Stiff Composite Material
An Examination of Uniformly Oriented Ultra-Thin High Modulus CFRP Tape Composite Material
MARCUS JOHANSEN
Department of Industrial and Materials Science
Chalmers University of Technology

Abstract

Lighter materials are needed to decrease fuel consumption in the transport industry. Conventional carbon fibre reinforced polymer composites have excellent stiffness-to-weight ratio, but are often discarded due to brittleness. This Master's thesis work investigates a new concept of carbon fibre reinforced polymer composite material, which can prove to be lightweight, ultra-stiff, exceptionally strong and easy to mass-produce. The new material consists of chopped ultra-thin tapes of very stiff carbon fibres held together by polymer. The tape pieces are randomly distributed to give in-plane isotropy through uniform orientation distribution. To allow for characterisation of this concept, the composite material was manufactured by tapes falling randomly through a channel onto a step-wise rotating substrate to build preforms, which were formed and cured by a heat press into plates. The plates were dissected and characterised through thermal and chemical analysis, cross-section microscopy, mechanical testing and fractography. The manufactured material shows great potential with a near isotropic behaviour, average stiffness of around 65 GPa and some measured tensile strengths in the vicinity of 500 MPa. The high tensile strength is found to depend on two competing fracture modes: tape pullout and fibre tension failure. In conclusion, the material concept is promising and with a refined manufacturing method we can soon see a new field of composite materials.

Keywords: lightweight, composites, discontinuous CFRP, uniform orientation distribution, in-plane isotropy, optical microscopy, tensile test, electron microscopy.

Acknowledgements

This Master's thesis was done at the Division of Material and Computational Mechanics at Chalmers University of Technology in collaboration with KTH Royal Institute of Technology, Oxeon AB, Volvo Cars and GKN Aerospace. I want to first thank my examiner and supervisor Leif Asp. Your guidance and enthusiasm has made this work fun and an enormous learning experience. Thank you Brina Blinzler, David Carlstedt, Dennis Wilhelmsson, Robert Hummerhielm and everyone else from Chalmers who lent their support. I also want to show special appreciation to Florence Rinn at Oxeon. You were invaluable for me to make the manufacturing work. Thank you Andreas Martsman, Fredrik Ohlsson and Oxeon for hosting me and providing material, manufacturing equipment and advises. At KTH, I am grateful for Dan Zenkert and colleagues for performing mechanical tests and finally I want to thank Fredrik Edgren representing Volvo Cars, and Spyros Tsampas and Adeline Kullerstedt representing GKN Aerospace.

Marcus Johansen, Gothenburg, May 2019

Nomenclature and Abbreviations

ν	Poisson's ratio
ρ_c	Composite density
ρ_f	Fibre density
ρ_m	Matrix density
σ_t	Tensile strength
E	Stiffness
E_p	Platelet stiffness
G_{II}	Mode II fracture toughness
l_p	Overlapping length of platelet
m_c	Composite mass
m_f	Fibre mass
m_m	Matrix mass
S_m	Matrix strength
t_p	Platelet thickness
v_f	Fibre volume fraction
w_f	Fibre weight fraction
w_m	Matrix weight fraction
X_G	Toughness based composite strength
X_S	Shear strength based composite strength
CFRP	Carbon Fibre Reinforced Polymer
DIC	Digital Image Correlation
DSC	Differential Scanning Calorimetry
FVF	Fibre Volume Fraction
FWF	Fibre Weight Fraction
SEM	Scanning Electron Microscope
UTHMT	Ultra-Thin High Modulus Carbon Fiber Reinforced Polymer Tape

Contents

List of Figures

List of Tables

1

Introduction

This introductory chapter is presenting the background to this Master's thesis and its relevance. Furthermore, a detailed explanation of the material concept studied is given and finally the aim, scope and specific issues under investigation are covered.

1.1 Background

In a time when lighter products are crucial for the transport industry to decrease energy consumption, lightweight materials with enhanced mechanical properties are highly sought after. Carbon fibre reinforced polymer (CFRP) composites, typically with continuous fibres, provide excellent stiffness-to-weight ratio and appear to solve the industry's conundrum. However, some of the drawbacks of this type of composite material are brittleness and difficulty to mass-produce. This Master's thesis work investigates a new concept of CFRP composite material, utilising discontinuous tapes with a uniform orientation distribution, which can prove to be lightweight, ultra-stiff, exceptionally strong and easy to mass-produce. Figure 1.1 shows a schematic representation of tapes with uniform orientation distribution.

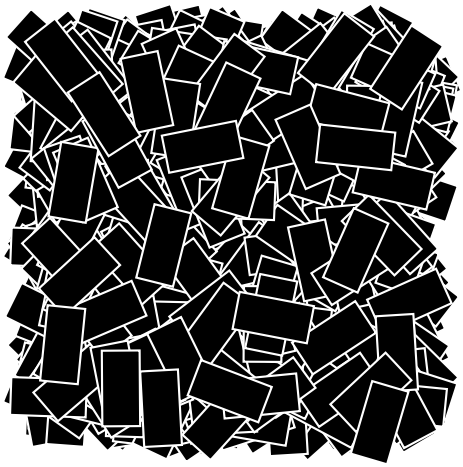

Figure 1.1: An illustration of 1000 randomly distributed CFRP tapes.

Previous work on discontinuous CFRP tape based composites has been done at the University of Tokyo and Imperial College London. Takahashi and colleagues showed that it is possible to manufacture in-plane isotropic composites based on discontinuous CFRP with good mechanical properties from randomly oriented pre-impregnated tapes. The tape used had a thickness of 50 µm and the fibres in the tape had a stiffness of 230 GPa. The composite material they produced had a stiffness of 50 GPa and strength of 500 MPa [2]. Pimenta and Robinson put forward a model implying that the strength of a composite with discontinuous inclusions in a brittle matrix increases with increased stiffness and decreased inclusion thickness [3]. This model is further explored in Section 1.2.

The uniqueness of the concept in this thesis compared to previous work is that instead of using fibres of standard modulus (200 to 270 GPa) and thin tapes (50 µm), fibres of high modulus (450 GPa) and ultra-thin tapes (22.5 µm) are used. This tape is referred to as ultra-thin high modulus carbon fibre reinforced polymer tape (UTHMT). According to Pimenta's and Robinson's model, the stiffness and thinness of UTHMTs in a polymer matrix promises to yield a high strength composite. At the same time, the high stiffness of UTHMTs supports a high total stiffness for the material. With the UTHMTs uniformly oriented in the plane of the composite, an in-plane isotropic material is expected.

This concept has now been targeted to be verified and characterised by this Master's thesis conducted at Chalmers University of Technology. The thesis is a part of a project collaboration between Chalmers, KTH Royal Institute of Technology, Oxeon AB, Volvo Cars and GKN Aerospace. The project started in October 2018. The responsibility of project leading, manufacturing and modelling falls on Chalmers and mechanical testing on KTH. Oxeon, Volvo and GKN are involved in all instances, however Oxeon is heavily contributing in the manufacturing segment and also provides material.

1.2 The concept in detail

Nature's structural materials are often superior to man-made ones. The lightweight material studied in this thesis is mimicking the structure found in natural composite materials such as nacre. Nacre, commonly known as mother of pearl, has a 'brick-mortar' structure where stiff platelets are embedded in a soft matrix. This structure yields excellent stiffness and strength [1]. The platelets can be considered as two-dimensional and carries load and gives stiffness, while the matrix transfers load through shear. The subject of this thesis work uses this material structure, but UTHMT as the two-dimensional platelet and polymeric material as matrix.

Pimenta and Robinson report on two competing models for predicting the strength of a 'brick-mortar' structured material, assuming that the platelets withstand the stresses and remain intact during loading. The first model is strength-based. The composite strength X_S then depend on the shear strength of the matrix S_m, the overlapping length of the platelets l_p and the platelets thickness t_p through:

$$X_S = \frac{l_p}{t_p} \cdot S_m. \tag{1.1}$$

The second model is toughness-based. The composite strength then depends on the mode II fracture toughness of the matrix G_{II}, the platelet stiffness E_p and the platelet thickness t_p by:

$$X_G = \sqrt{\frac{2 \cdot E_p \cdot G_{II}}{t_p}}. \tag{1.2}$$

The property deciding which response is active for a certain material is, according to Pimenta and Robinson, the thickness of the platelets. For thick platelets a plasticity dominated response is active, while for thin platelets the response is instead dominated by fracture mechanics [3]. So if a platelet is sufficiently thin, a 'brick-mortar' structured material is behaving in accordance to Equation 1.2. If the platelet then is allowed to become even thinner and the stiffness of the platelet increases, the strength of the whole material increases. In other words, a 'brick-mortar' structured material with ultra-thin, high modulus platelets will give high strength. At the same time, the high modulus of the platelet will provide a high overall stiffness for the material.

The concept in focus for this thesis is applying a 'brick-mortar' structure with UTHMTs as platelets to yield a rarely seen combination of high stiffness, high strength and low weight. Furthermore, the

concept includes the UTHMTs to be uniformly oriented in the composite. Hence, in-plane isotropy will occur, contrasting the famous anisotropy of continuous CFRP composites. Processability of the high modulus fibre is achieved by the tapes sliding relative to each other during press forming. This concept promises to revolutionise the use of CFRP in the transport industry. Nonetheless, the concept is still to be verified.

1.3 Aim

The purpose of this thesis is to show that an in-plane isotropic high stiffness and high strength lightweight composite material is achievable with the concept of uniformly oriented UTHMTs. It is required that the material is manufactured and the material properties are characterised.

1.4 Scope

To keep the project focused some boundaries are set up. The manufacturing development will include production of test specimens of highest achievable quality within the time frame of the project. Further investigation into the optimal manufacturing method or an economical study of manufacturing methods is beyond the scope of this thesis. The characterisation of material properties through mechanical testing will be restricted to tensile tests.

1.5 Specific issues under investigation

- What degree of isotropy can the manufactured composite achieve?
- What stiffness and strength can the manufactured composite achieve?
- What are the mechanisms behind the manufactured composites stiffness and strength?

2

Manufacturing

To verify that a uniformly oriented UTHMT composite exhibits the predicted properties, the composite itself first has to be manufactured. The following sections describe the process from tape to plate.

2.1 Materials

The material components used in this thesis work are carbon fibres embedded in thermoset matrix. Two fibre types are used, MR70 and HS40. In Table 2.1 the material properties for these fibres are presented. MR70 fibre is classed as *Intermediate modulus*, while HS40 is classed as *High modulus*. At Oxeon the fibres are spread to a tape with thickness 0.0225 mm and width 20 mm and sprayed with an epoxy resin system based on bisphenol-A developed by Oxeon. This resin is referred to as reactive binder BI018 and is used for composites with low resin content. It is stable against curing for temperature below 80 °C. In Table 2.2 properties of reactive binder BI018 are presented. Note that mechanical properties for the cured polymer are not available. Two batches of BI018 are used in the thesis work. The second batch is slightly modified to allow for better resin flow and higher glass transition temperature.

Table 2.1: Properties for the fibre types MR70 and HS40.

Fibre type	Density, ρ_f [g cm^{-3}]	Stiffness, E [GPa]	Strength σ [MPa]
MR70	1.82	325	7000
HS40	1.85	425	4610

Table 2.2: Properties for reactive binder BI018.

Resin type	Density, ρ_m [g cm^{-3}]	Cure temp., T [°C]	Cure time, t [min]
BI018	1.15	150	60

When spread and sprayed, the tape is rolled up on bobbins. Over the course of the thesis work, four different tapes were produced, see Table 2.3. Tape type 1 with HS40 was initially used but was quickly discarded since it fell apart or folded very easily. Type 2 with MR70 proved to be much more uncomplicated to handle and was used for calibration of the manufacturing process. However, to verify the concept, higher fibre stiffness was required. Therefore HS40 fibre was used in conjunction with the second batch of resin in type 3. Type 3 was more sturdy than type 1, but type 1, type 2 and type 3 all had in common that they were sprayed with resin on only one side. This led to dry pockets in the composite material where two dry tape sides were facing each other. To mitigate dry pockets, tape type 4 was sprayed on both sides. Type 4 was the final tape type to be used.

Table 2.3: Tape types.

Tape	Fibre	Resin batch	Double sprayed	Resin weight fraction [%]	Thickness [µm]
1	HS40	1	No	38	22.5
2	MR70	1	No	38	22.5
3	HS40	2	No	38	22.5
4	HS40	2	Yes	45	22.5

2.2 Lay-up

One of the most crucial parts is the lay up of UTHMTs. The goal is to ensure a uniform in-plane tape orientation. Additionally, an even thickness in the lay-up is important. Earlier lay-up methods have been manual placement according to computer generated random patterns [4] and wet-type paper making process [5]. These methods are very time consuming. In 2015 Darvell performed several tests to determine the best method for lay-up of uniformly oriented tapes. The most promising method identified was a method in which the tape pieces fall through a channel and shuffle before landing randomly on a substrate [6]. This lay-up method was used and how it is performed is outlined below.

Firstly, the tape is provided on a bobbin, which is mounted to be able to spin so tape is unwound. The tape is then fed into a chopper. Tension in the fibre is generated by the pull of the chopper and braking of the bobbin. Wrinkling of the tape is avoided by placing a roll in front of the slit entering the chopper, see Figure 2.1.

In the chopper, Chopcot T5 from Van der Mast, there are three rotating components: pressure roll, stress roll and blade roll. The tape is pressed by the pressure roll onto the stress roll, which pulls the tape to the blade roll. The blade roll has a diameter of 75 mm and is fitted with six blades. This setup gives six tape pieces per revolution with the respective length of 40 mm. The chopper is run at a speed of 100 rpm, correlating to a tape consumption rate of $0.4\,\mathrm{m\,s^{-1}}$.

From the chopper the tape pieces fall freely down through a fall channel with square cross-section 300 mm by 300 mm and onto a substrate, building a square shaped preform. During the fall the tapes are shuffled around by the air resistance and land flat with a random orientation. With thousands of randomly oriented tapes an overall uniform fibre orientation is expected. The theoretical number of layers of tape for a plate with thickness 0.5 mm and tape thickness of 0.0225 mm is 22 layers. However, the uniformity of thickness is dependent on the tape pieces' falling positions. This is problematic if tape pieces fall at one position more easily than at other positions. For a static setup of chopper and falling channel it is most likely that some falling positions will be more frequent. To mitigate this, the substrate is rotated several times while building the preform, see Figure 2.2. For example when building a 0.5 mm thick preform the chopper is first on for 30 s building the first layers of the preform. The first layers are lightly consolidated with low temperature and pressure. Then the substrate is turned 180°, the chopper is on for another 30 s and the new layers are consolidated on top of the first layers. This is done in total eight times and the substrate orientation is 0°, 180°, 90°, −90°, 0°, 180°, 90° and −90°. It is also important to prevent edge effects and this is done by placing the fall channel more than a tape length, 40 mm, above the substrate. This to prevent the tapes standing on one edge and leaning on the fall channel wall. Furthermore, edge effect is avoided by manufacture larger preform than the planned final size of the pressed plates. Lastly, the preform is debulked in a lamination machine with a temperature of 60 °C and pressure of 3 bar.

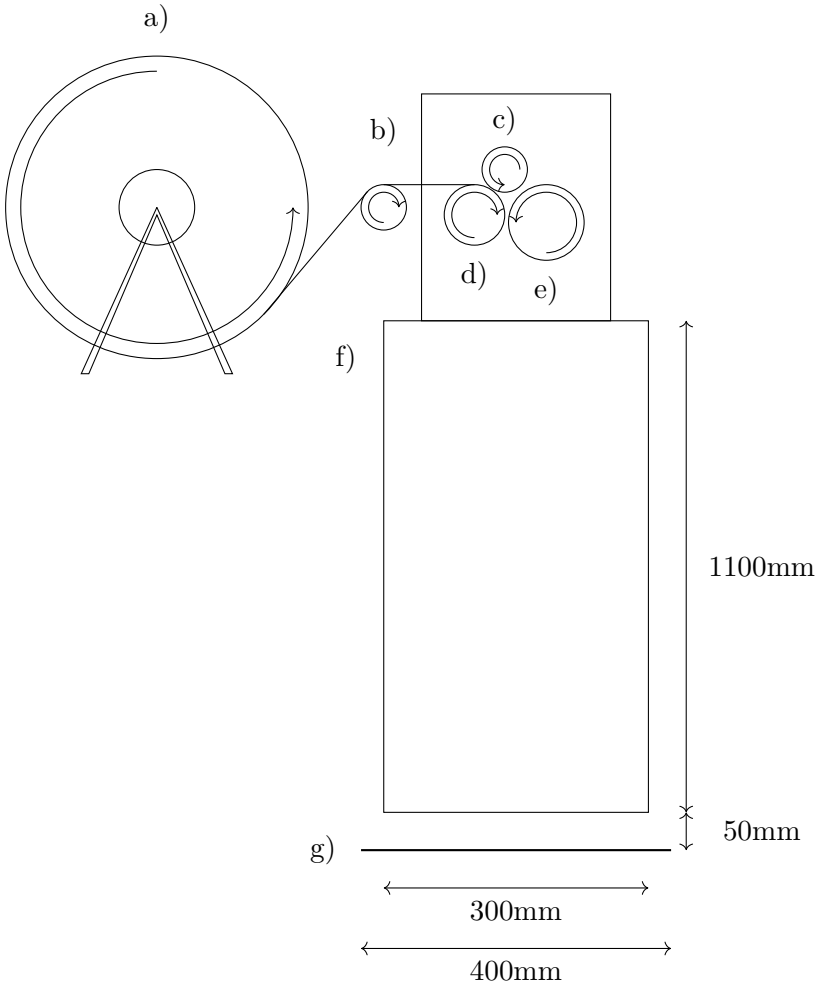

Figure 2.1: A schematic representation of the chopper setup. a) bobbin, b) stabiliser, c) pressure roll, d) stress roll, e) blade roll, f) falling channel g) substrate.

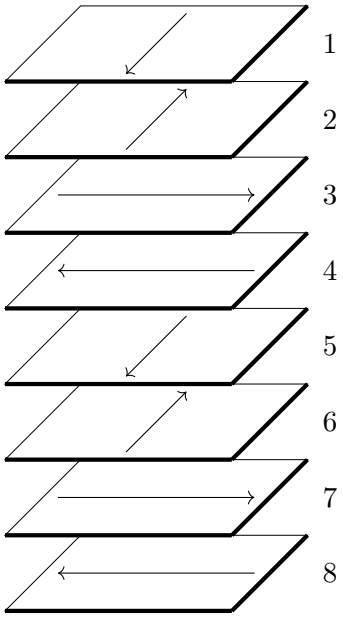

Figure 2.2: The rotation scheme to mitigate accumulation of tapes at favoured positions. In total, eight rotations are performed.

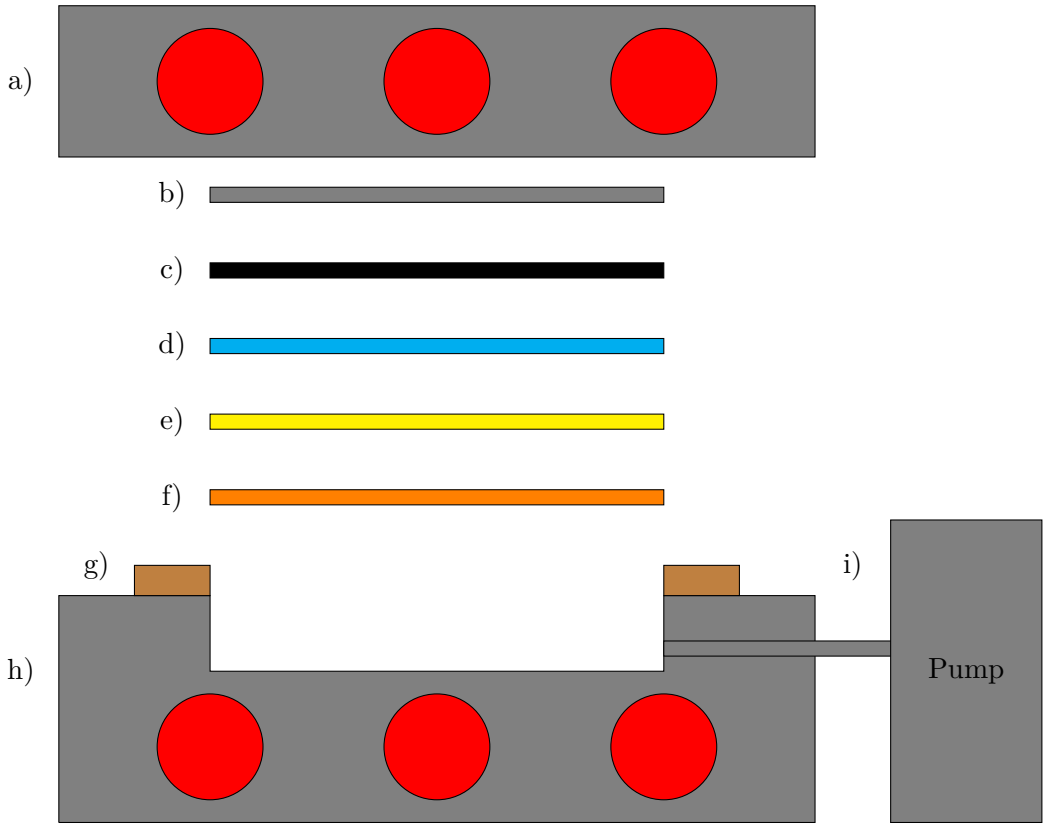

Figure 2.3: Schematic representation of the heat-press tool with a) top heat block, b) aluminum cold plate, c) UTHMT composite plate, d) perforated silicone film, e) breather, f) pressure distributing silicone rubber, g) sealing tacky tape h) bottom heat block and i) vacuum pump.

2.3 Forming

The final step in the manufacturing of the UTHMT composite plate is the pressing and curing. This makes sure that the fibres become sufficiently wetted by the resin and the resin is completely cross-linked.

The tool used for forming in this thesis work is a heat-press consisting of a top and a bottom block with integrated heating elements, see Figure 2.3. The top and the bottom have independently programmed heat cycles. The two blocks are held together with 20 bolts and nuts. These bolts and nuts are also used for the pressing action of the tool. By calculating the number of turns per bolt a targeted pressure can be reached. During a cure cycle a combination of automated and manual actions therefore occur. The heating is governed by the programming and so is automated, while the pressure is controlled by tightening and loosening the bolts by hand.

The initial step in forming is to cut the uncured preform produced with chopper and fall channel to fit the heat-press's cavity, 275 mm by 275 mm. When press forming, it is of importance to generate a liquid pressure on the resin to generate resin flow to wet the fibres. Therefore the preform is cut so the whole cavity is filled. Then the contact surfaces of the heat-press are treated with a release agent to prevent adhesion.

In the bottom of the cavity a pressure distributing silicone rubber is placed so the applied pressure over the whole preform becomes even. On top of the rubber is first a breather and then a perforated silicone paper and the preform placed. The breather is connected to an outlet at the edge of the cavity, which in turn is connected to a vacuum pump. Around the cavity tacky tape is applied. Finally, a cold plate of aluminium is placed on the preform and then the top block is bolted to the bottom block. To suppress formation of pores and air bubbles in the material the vacuum pump is turned on. The

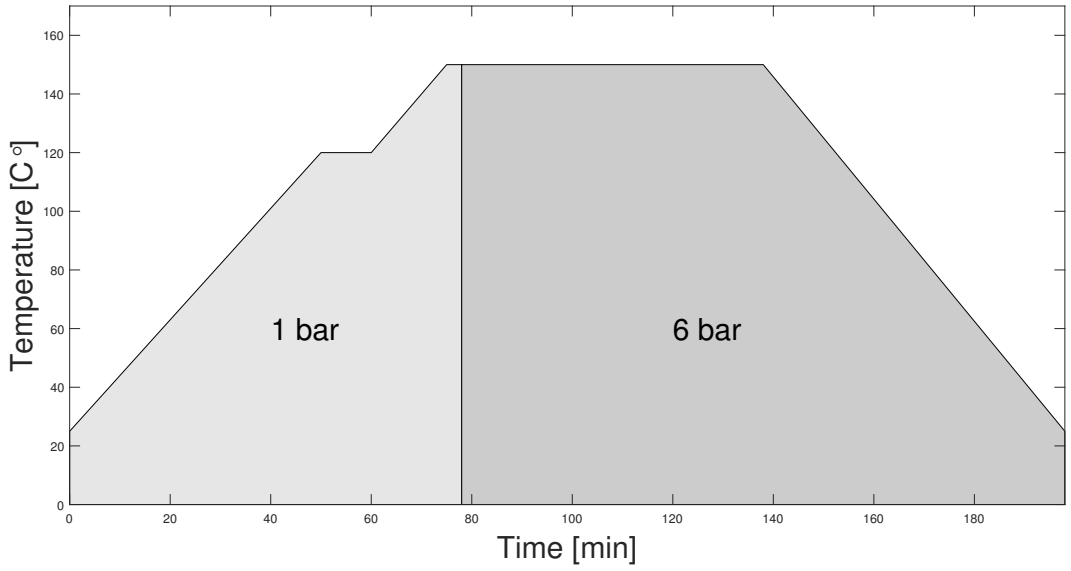

Figure 2.4: Diagram of the cure cycle.

tacky tape seals the heat-press, the breather distributes the vacuum evenly over the preform and the perforated silicone film partially restricts the resin to flow straight to the outlet.

By tightening the bolts a pressure of 1 bar is applied. The top and bottom blocks are heated according to the same programming, see Figure 2.4; ramp up 2 °C min^{-1} from room temperature to 120 °C and hold for 10 min; ramp up 2 °C min^{-1} to 150 °C and hold for 3 min; apply 6 bar and hold 1 h; cool to room temperature and relieve pressure. This cure cycle is recommended by Oxeon.

When the UTHMT composite plate is cured the vacuum is turned off, the bolts are loosened and the blocks are separated. Thanks to the release agents on the press surfaces the plate is easily extracted and then the edges are trimmed. The plate is now ready to be examined.

2.4 Evaluation

To improve the manufacturing the UTHMT composite is evaluated with several methods. These are discussed more in depth in Chapter 3. Aspects evaluated are: degree of cure, degree of fibre wetting, fibre volume fraction, thickness uniformity and tape orientation uniformity.

Degree of cure is preferably evaluated with *Differential Scanning Calorimetry*, see Section 3.1. As long as the DSC analysis does not reveal any exothermic spikes or bumps a fully cured specimen can be assumed. Fibre volume fraction is measured with *Matrix Digestion*, see Section 3.2.

The degree of fibre wetting is analysed by optical microscopy of the plate cross-section, see Section 3.3. Magnified images of cross-sections are photographed and studied. Wetting of fibres is qualitatively judged based on if the fibres appear to be encapsulated by matrix or not. With an image processing program the volume fraction of pores can be approximated and provide a quantitative value of wetting. Rudimentary visual inspection of the surface of the plate also gives a general sense of wetting. A combination of shiny and dull surfaces most likely indicates dry fibres.

Uniformity of thickness is manually measured with a caliper. Several positions on the plate is measured. The smaller the scatter of thickness, the higher the uniformity. Care must be taken so that the thinnest positions are measured correctly by avoiding the caliper head to get stuck on adjacent tapes.

Finally, the tape orientation uniformity is probably the most difficult aspect to evaluate. A visual inspection of the surfaces can tell if a major favouring of orientation has occurred. However, this does not give any information about the bulk of the plate. To evaluate the bulk, tensile tests, see Section 3.4, can be performed in multiple directions. If an isotropic response is produced, then uniform tape orientation is proven.

3

Characterisation

Different characterisation methods are used to explain the mechanisms behind mechanical properties and to evaluate manufacturing. These methods are explored in this chapter and include the thermoanalytical method of Differential Scanning Calorimetry, the chemical analysis Matrix Digestion, Tensile Test, Stereo- and Compound Microscopy and Scanning Electron Microscopy.

3.1 Thermal analysis

In a DSC experiment heat flow is measured as temperature is controlled and changed. The result is a curve of heat flow versus time. DSC can be used to verify that a thermoset matrix in a composite material is fully cured [7]. Samples are cut to small dimensions, around 3 mm by 3 mm, to fit the crucible of the calorimeter. The device is then programmed to follow a temperature curve starting at room temperature and ramping up 10 °C min^{-1} to 190 °C and then back to room temperature, see Figure 3.1. When later studying the heat flow-time curve one is on the look out for a distinct change in heat flow in the form of a bump on the curve. The presence of distinct variation in heat flow indicates that a exothermic or endothermic reaction has occurred during the experiment. If so, it can be assumed that the recorded reaction is the cross-linking of the thermoset, meaning that the matrix was not cured before the experiment. Likewise, if no sudden change in heat flow is seen, then the matrix was fully cured before the experiment.

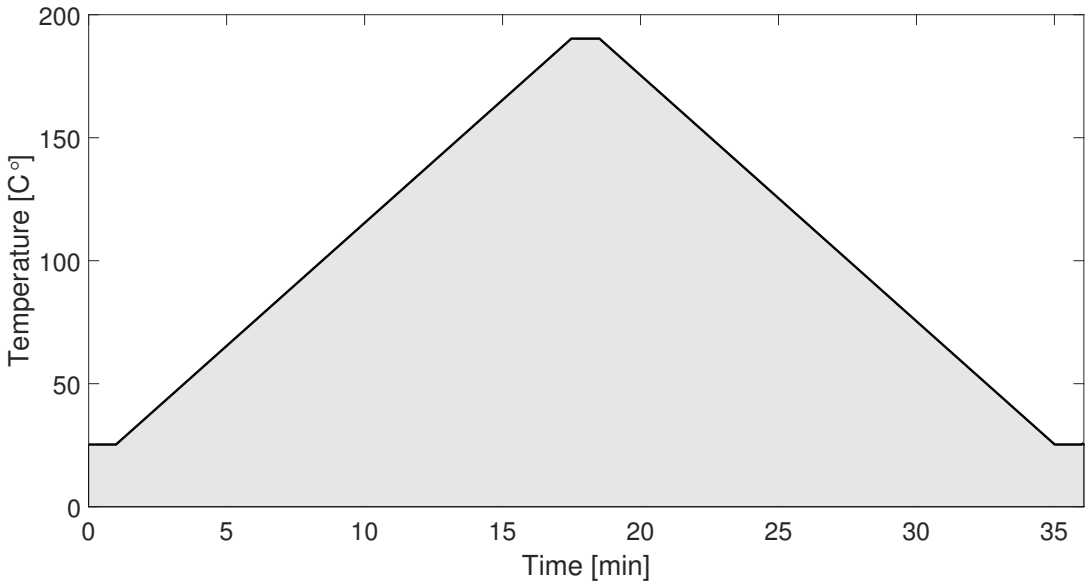

Figure 3.1: Temperature program for DSC.

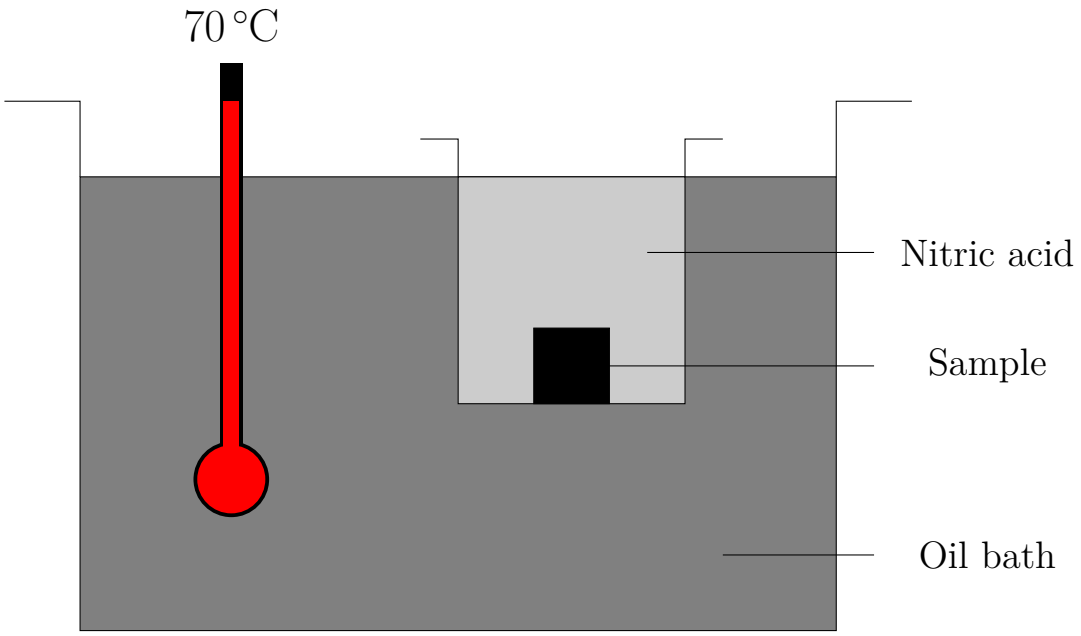

Figure 3.2: Schematic representation of the setup for matrix digestion.

3.2 Chemical analysis

To determine the fibre volume fraction in the UTHMT composite material, matrix digestion with nitric acid is performed according to ASTM Standard D3171 [8]. Samples are cut out and weighed to nearest 0.0001 g. The samples are then submerged in a container with nitric acid (NHO_3). The container is held at 70 °C by an oil bath, see Figure 3.2. Nitric acid is very oxidising and the epoxy matrix is dissolved over 5 h. Finally, the remaining fibres are washed with distilled water and acetone, dried for 24 h and weighed to nearest 0.0001 g. With the total composite mass m_c and fibre mass m_f measured the the fibre weight fraction is calculated by:

$$w_f = \frac{m_f}{m_c}. \tag{3.1}$$

Then with fibre density ρ_f and matrix density ρ_m the fibre volume fraction is calculated through:

$$v_f = \frac{1}{1 + \frac{\rho_f}{\rho_m}(\frac{1}{w_f} - 1)}. \tag{3.2}$$

3.3 Cross-section analysis

From analysis of the cross-section of UTHMT composite plates information regarding fibre wetting, fibre volume fraction and fibre orientation can be obtained. The cross-section surface is ground and polished before examination with a compound microscope and image processing software.

The sample preparation si initiated with samples cut from the plate to a dimension of 10 mm by 10 mm. The samples are mounted in an epoxy resin using the vacuum impregnation unit CitoVac from Struers. The resin is cured in an oven at 75 °C for 1.5 h. When cooled, the resin mounted samples are ground with TegraPol-31 and TegraForce-5 from Struers with increasingly fine papers: 500, 800, 1000, 1200 and 2000. Then the same machine is used to polish the samples with a cloth and 1 µm polishing liquid. Finally the samples are cleaned with ethanol.

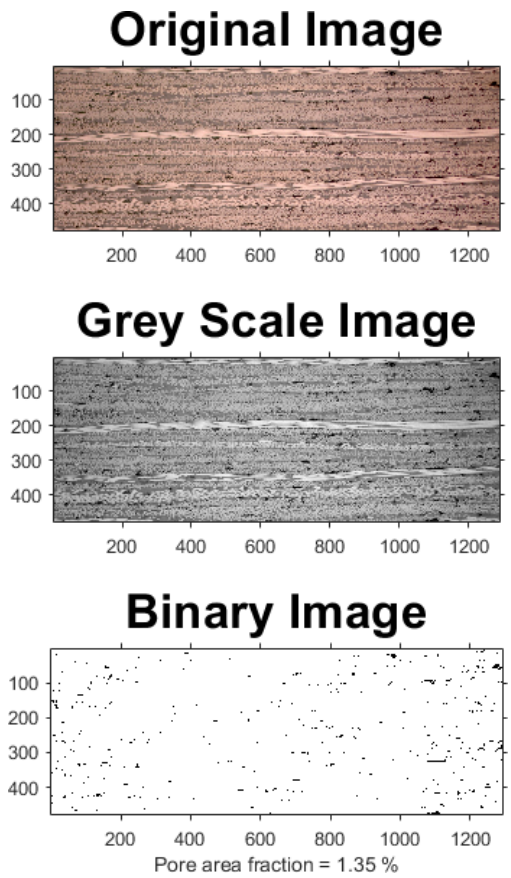

Figure 3.3: Original image translated into a grey scale and a binary image.

The samples are studied with the compound microscope Leica DMRX and images are taken using AxioCam MRc5 and the program AxioVison. To approximate the amount of porosity, an image processing code in MATLAB is used. The code first translates the images taken with the compound microscope to a grey scale image. Then a binary image is created with a threshold to separate white and black pixels, see Figure 3.3. White pixels are assigned the value 1 and correspond to presence of material, while black pixels are given the value 0 and correspond to pores. The ratio of black pixels divided by total amount of pixels gives and approximation of the porosity.

3.4 Tensile test

Evidently, mechanical testing is the major method to characterise the mechanical properties of a material. Normally test standards, such as ASTM Standard D3039 [9], are employed when performing mechanical testing on polymer matrix composite materials. However, with a specimen thickness of 0.5 mm used in this thesis work there is no applicable standard and therefore the following procedure is performed.

For the tensile test an UTHMT composite plate with thickness 0.5 mm is cut into long rectangular specimens of dimensions 100 mm by 25 mm. Three directions are cut: 0°, 45° and 90°, see Figure 3.4. Specimens directly from the edges of the plate are avoided, so that edge effects stemming from the manufacturing is prevented. An average thickness of each specimen is measured. The cut sides of the specimen are polished with sandpaper and tabs are applied at the specimen ends to protect the composite when clamping it in the tensile test machine, see Figure 3.5. The tabs are glass fibre reinforced epoxy glued to the specimen with Araldit 2015. Figure 3.5 also shows the setup of the tensile test machine, an Instron 5567, with a load cell with capacity up to 30 kN. On the back of the specimen an extensometer is placed and held with rubber bands. The load of the test machine

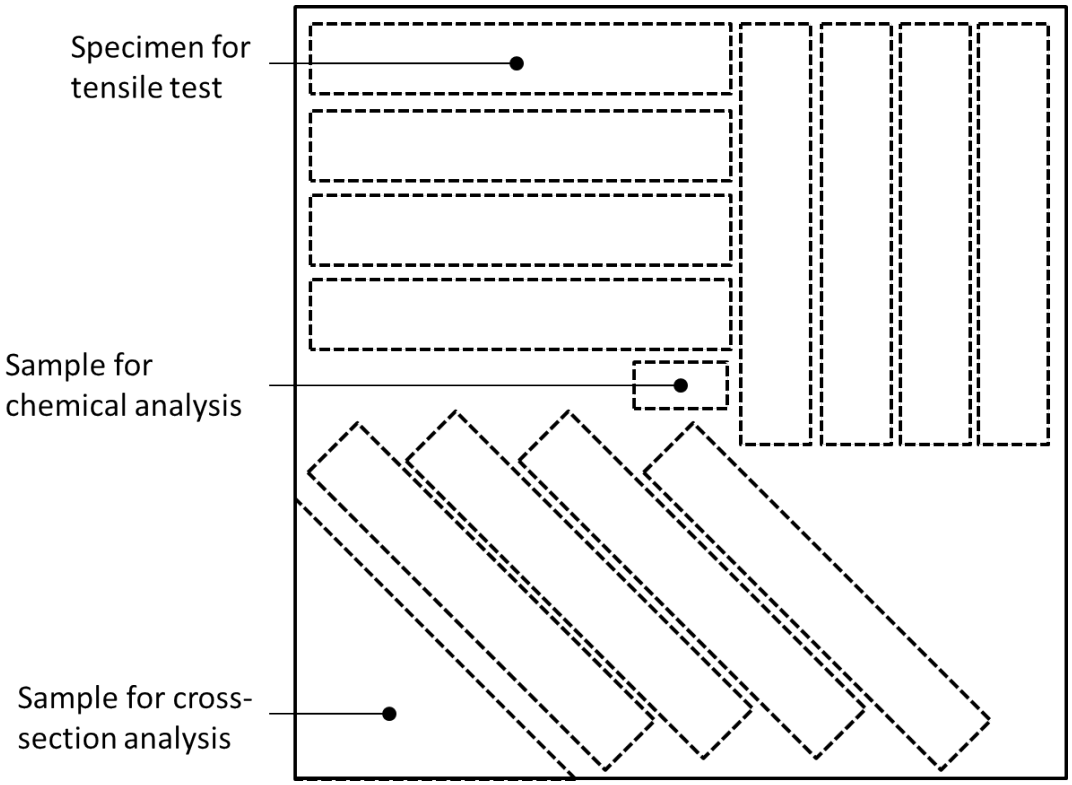

Figure 3.4: The cutting pattern of specimens and samples from an UTHMT composite plate.

and displacement of the extensometer is recorded with the software Cyclic. On the front surface, the specimens are sprayed with white paint forming a random pattern. This pattern allows the Digital Image Correlation (DIC) cameras to record the strain on the surface of the specimen. The setup of the DIC cameras can be seen in Figure 3.5. From the recorded images the DIC software ARAMIS 6.3 calculates the strain. The tensile test gives data for tensile strength (σ_t), stiffness (E_x, E_y, E_{45}) and Poisson's ratio (ν_{xy}).

Figure 3.5: The left picture shows the DIC-cameras mounted in front of the tensile test machine, in the middle picture is a specimen clamped in the tensile test machine and the right picture depicts four tabbed specimens ready for testing.

3.5 Fractography

To characterise failure mechanisms fractography of the fractured specimens from tensile testing is performed. The principal procedure of failure analysis [10] is followed in this thesis work, see Figure 3.6. The aim of the fractogrphy is identified as characterise failure mechanisms of UTHMT composite under tensile load.

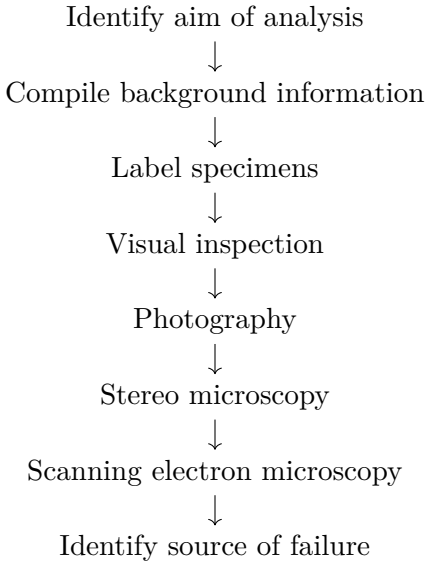

Figure 3.6: Principal failure analysis procedure.

The first step is visual inspection where fracture location and features are noted. The appearance of the fractures are documented with photographs. When visual inspection and photography of the fracture surface is completed higher magnification is required and microscopy is utilised. Instead of the compound microscope mentioned in Section 3.3, the stereo microscope ZEISS SteREO DiscoveryV20 is used owing to the stereo microscope's large depth of field. A large depth of field is useful when examining uneven surfaces as fractures. Firstly, the fracture is studied with low magnification to build a general sense of the position of the main features. Images of the fracture are taken with AxioVision. Following the initial sweep the fracture is examined in more detail by zooming periodically as the fracture surface is orderly scanned. To achieve a non-biased analysis, searching for specific failure modes or directions is avoided. Furthermore, by independent examination of matching fracture surfaces findings can be verified.

Some features are not visible with the magnification of a stereo microscope and then scanning electron microscope is the next step. An XL30 ESEM from Philips is used. The chamber of the SEM limits the size of the specimen and therefore some minor preparation is performed. A cut parallel and close to the fracture surface separates the fracture zone from the bulk of the specimen. Care is taken not to alter the fracture surface. Since electrons are impinged on the fracture surface during a SEM session, the material must be electrically conductive, else risking to overcharge and damage the surface. Carbon fibres are conductive, but the matrix is not. This is solved by sputtering the surface with gold coating with Edwards S150B Sputter Coater. Finally, the specimen is mounted in the SEM chamber and methodical scanning along the fracture surface is commenced. When all data has been collected conclusions regarding the failure mechanisms are drawn.

4

Results

The results from manufacturing and the characterisation methods are presented in this chapter. The final version of the produced composite material is presented first, followed by thermal and chemical analyses where degree of cure and fibre volume fraction are covered. The cross-section analysis shows micro structures and the results from tensile test provide information on stiffness, strength and strain to failure. Finally, the fractography covers the different fracture modes of the material.

4.1 Manufacturing

After several iterations a final manufacturing method was established. HS40 fibre tapes with reactive binder sprayed on both sides was used. From this method two plates, no.1 and no.2, were manufactured. Except chemical analysis, the results below comes from testing of these two plates. The two plates were manufactured to dimensions of 278 mm × 278 mm × 0.5 mm and had a mass of 65 g and 67 g. The top side and the bottom side of plate no.1 are depicted in Figure 4.1. A difference in surface finish can be seen, where the top side is smooth since it engaged with the aluminium cold plate during pressing. The bottom side is much more uneven since it was pressed against the silicone rubber.

Figure 4.1: Juxtaposition of the top side (left) and bottom side (right) of plate no.1.

4.2 Thermal analysis

The cure cycle used in manufacturing of the UTHMT composite does cure the reactive binder BI018. From the DSC experiment, data for three different materials are presented in the Heat flow versus Time

diagram in Figure 4.2. The materials are two references and a sample from the UTHMT composite. The references are an uncured and cured material. The uncured material yields a pronounced bump on the curve indicating reaction and curing. However, the tested sample closely follows the cured reference material and no reaction occurs.

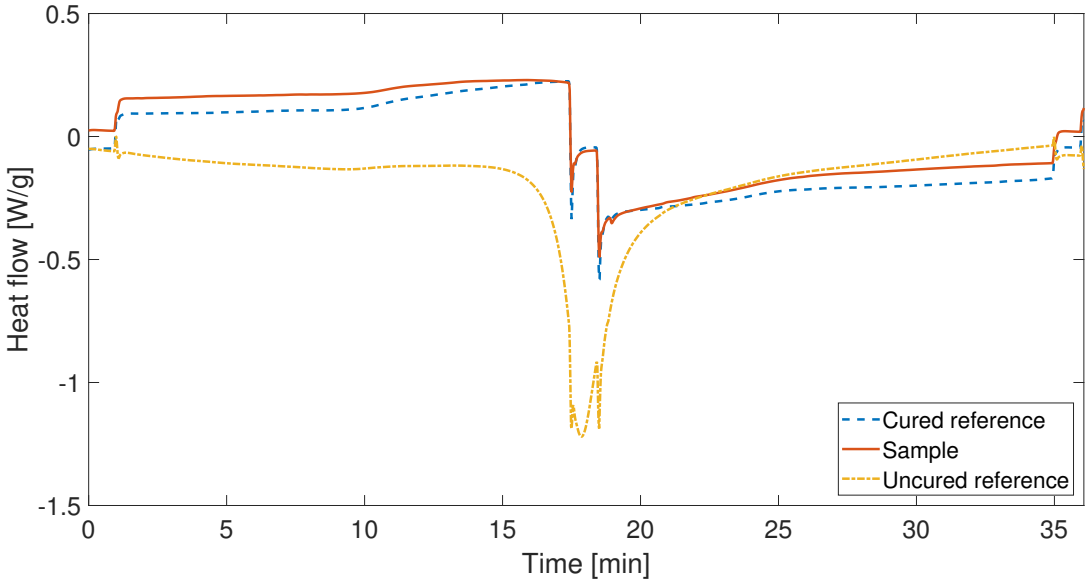

Figure 4.2: DSC results for a cured and an uncured reference material compared with a sample from an UTHMT composite.

4.3 Chemical analysis

For matrix digestion three samples were taken from each plate, no.1 and no.2. In Table 4.1 following are reported: measured sample mass before digestion m_c, measured sample mass after digestion m_f, calculated fibre weight fraction w_f and calculated fibre volume fraction v_f. The FVF ranges from 43.65% to 49.68%. The average FVF for each plate is presented in Table 4.2. Plate no.2 has higher average FVF, 47.71%, than plate no.1 with 44.09%.

Table 4.1: Measured and calculated values from matrix digestion.

Plate no.	Total mass, m_c [g]	Fibre mass, m_f [g]	FWF, w_f [wt%]	FVF, v_f [%]
1	.3576	.1984	55.48	43.65
1	.2812	.1602	56.97	45.15
1	.3152	.1743	55.30	43.47
2	.4817	.2956	61.40	49.68
2	.3188	.1792	56.21	44.38
2	.3971	.2413	60.77	49.05

Table 4.2: Average fibre volume fraction in plate no.1 and no.2.

Plate no.	Average FVF, v_f [%]
1	44.09
2	47.71

4.4 Cross-section analysis

The porosity in the manufactured composite has been greatly reduced over the course of the thesis work. The porosity of an early produced UTHMT composite plate compared with the final version is presented In Figure 4.3. The black/white pixel ratio is approximately 6 percentage points lower in the final version, meaning that the manufacturing drastically has improved. Though there are still pores, the presence of larger pores is almost none.

The thickness of the plates varies with about 0.2 mm. The measured thickness at nine positions on plate no.2 is illustrated in Figure 4.4. This thickness variation of course depends on the number of layers stacked tapes, but the amount of resin between said layers does also vary and influences the thickness. An extreme case of this is seen in Figure 4.5. The thickness changes from 630 µm to 775 µm, but the number of layers are the same. This means that the thickness is not only dependent on the number of layers. The actual number of layers in a 0.5 mm thick plate is slightly lower than the theoretical number of layers. Figure 4.6 presents a cross-section with the targeted thickness, 500 µm. This cross-section has 18 layers which is 4 layers fewer than the theoretical number of 22.

The layers do not always lay completely flat and a wavy feature can then be seen. This is due to the layer being skewed by tape edges. A case of layer waviness is presented in Figure 4.7. In the figure four tape edges are present (marked with dots). The most curved layer (marked with a red line) is skewed between these tape edges. The effect of tape edges is not only skewing of layers, but they induce the formation of resin pockets. This happens both at the shorter and longer side of the tapes. Figure 4.8 and 4.9 show the regions around tape edges at fibre ends and parallel to the fibres, respectively. Pockets of resin are seen in both regions.

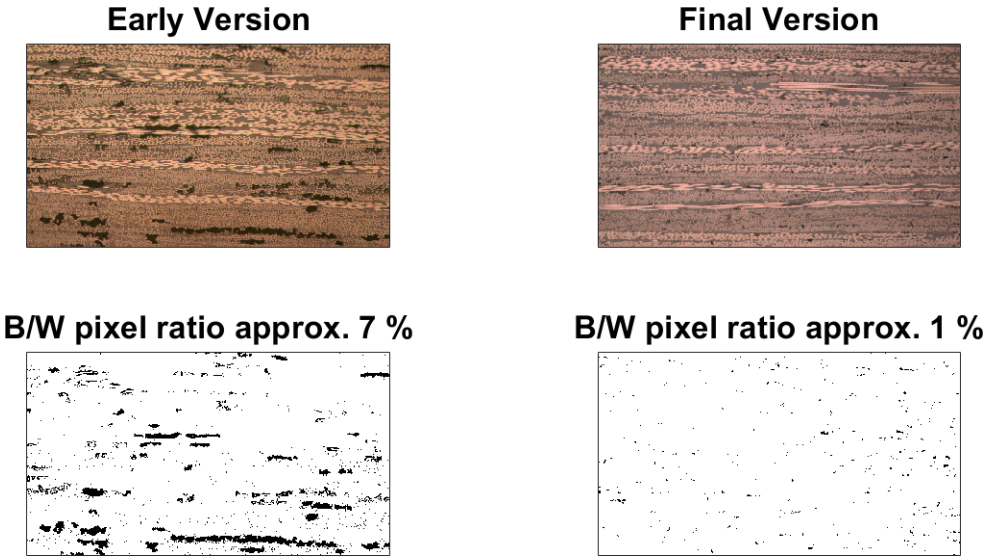

Figure 4.3: Comparison of cross-section and porosity between an early produced plate and the final version.

0.773	0.670	0.695
0.551	0.554	0.735
0.761	0.519	0.554

[mm]

Figure 4.4: Measured thickness at nine positions on plate no.2.

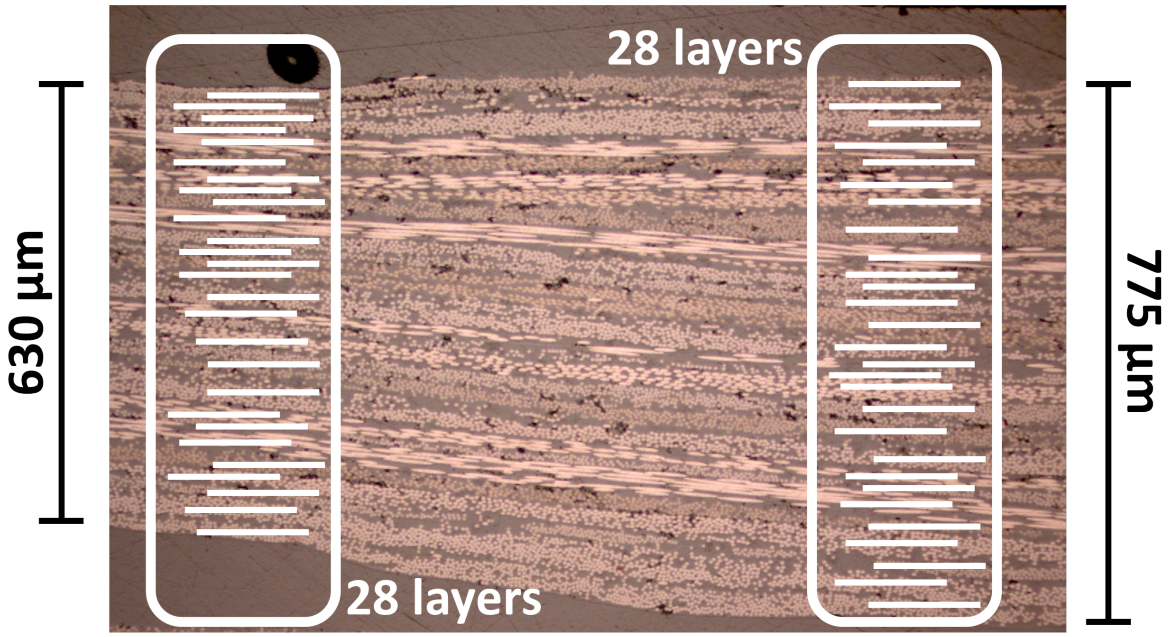

Figure 4.5: A cross-section with varying thickness from 630 µm to 775 µm, but with fixed amount of layers. The white lines inside the market region indicate each layer in that region.

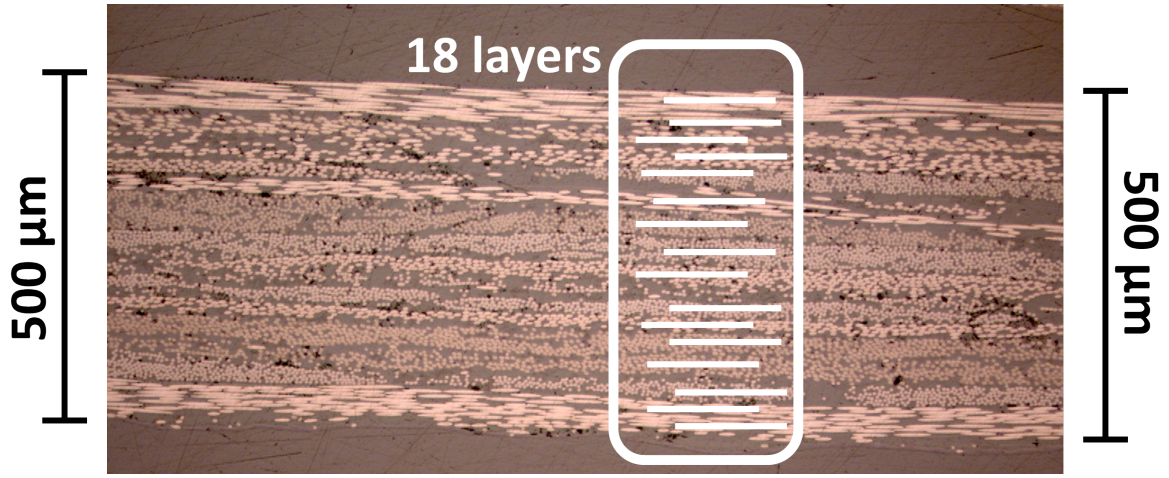

Figure 4.6: A cross-section with 18 layers.

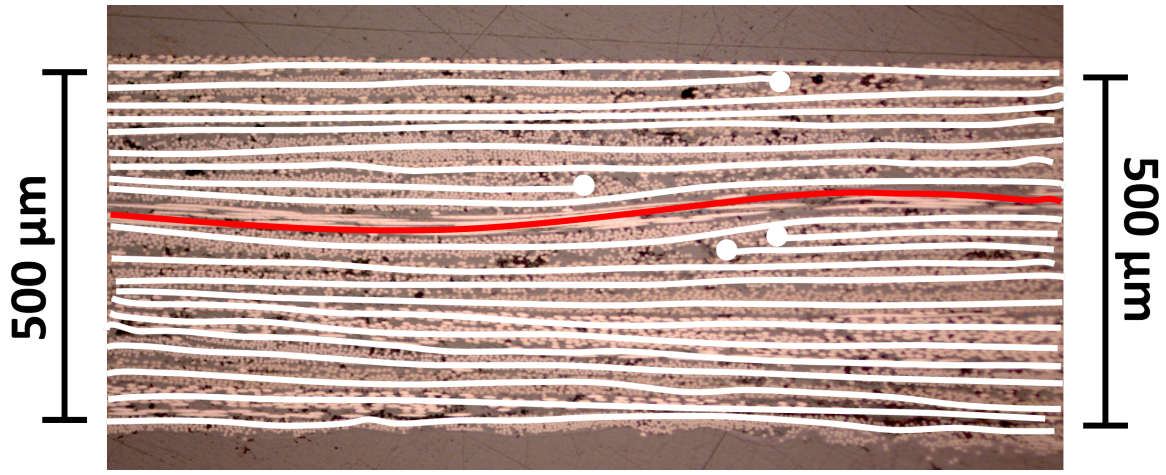

Figure 4.7: A cross-section with wavy pattern of layers. The white lines indicate layers. The red line indicates a specifically curved layer with fibre direction parallel to the cross-section. White dots indicate tape edges

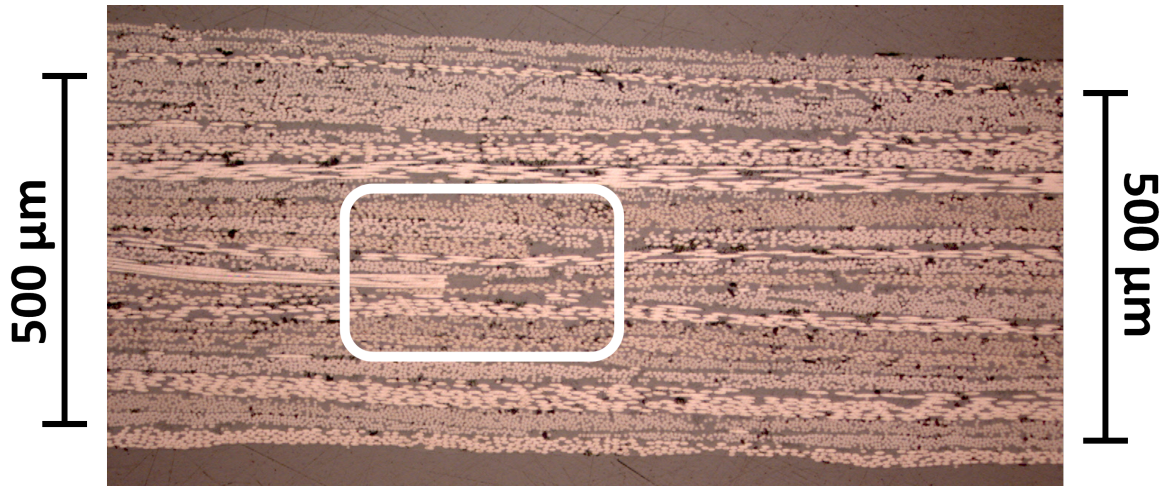

Figure 4.8: A cross-section with the region around a tape edge marked. The tape edge is at the fibre ends where the tape has been cut.

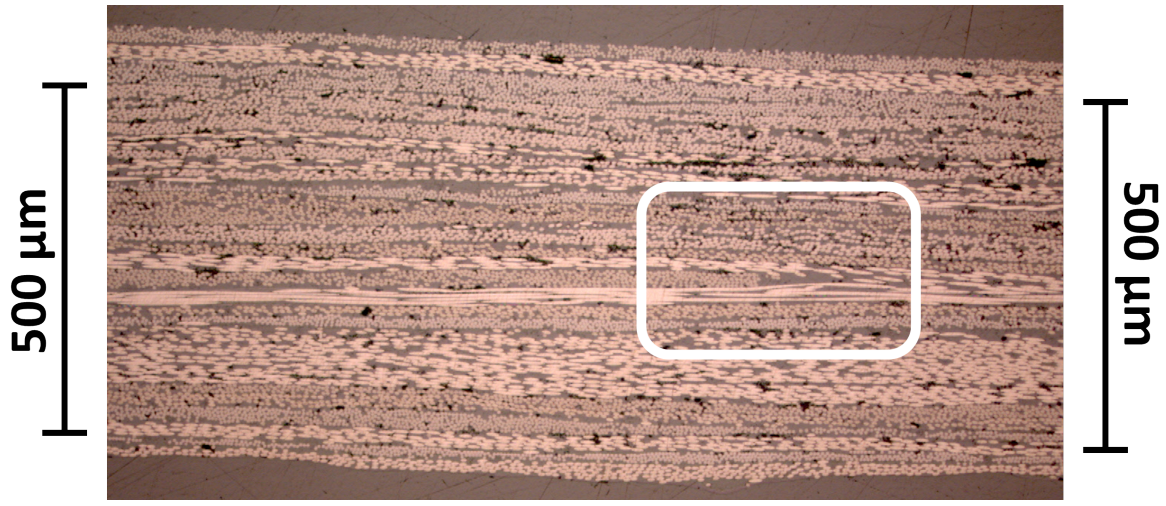

Figure 4.9: A cross-section with the region around a tape edge marked. The tape edge is parallel to the fibres.

4.5 Tensile test

The manufactured UTHMT composite material displays average stiffness in range of 65 GPa. The measured stiffness from the tensile test is presented in Figure 4.10 and 4.11. The average stiffness for plate no.1 is 62.6 GPa and for plate no.2 65.8 GPa. However, some specimens even show a stiffness above 85 GPa. The measured values show scattering where stiffness range around 35 GPa, and a slight trend of orientation influencing the stiffness can be seen. For example, the stiffness in plate no.2 increase when the orientation shifts from 90° to 45° to 0°.

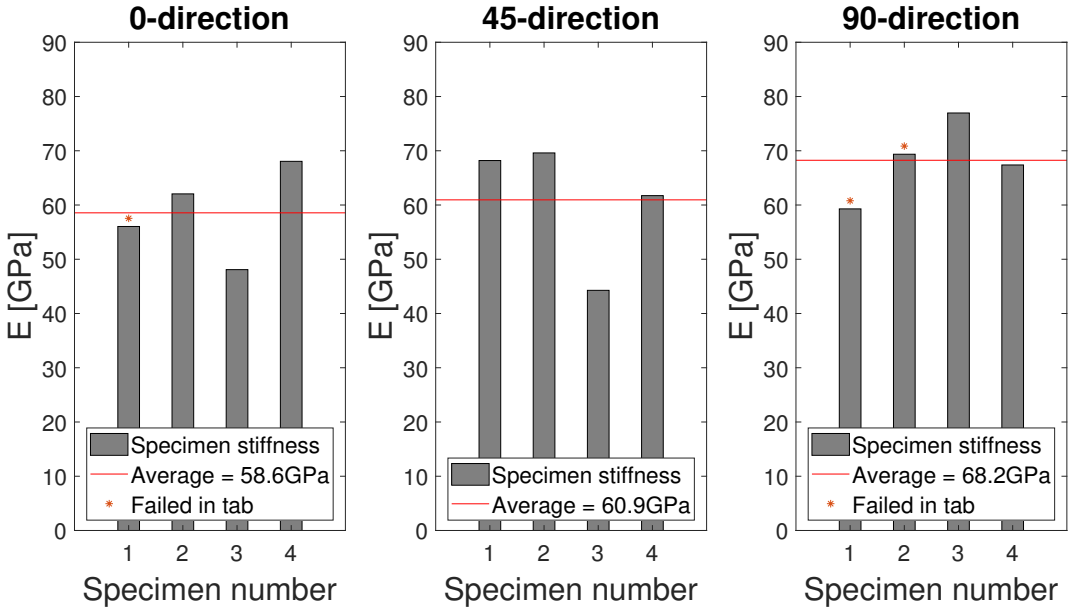

Figure 4.10: Measured stiffness in plate no.1 for three directions. Specimens which failed in tab are marked with an asterisk.

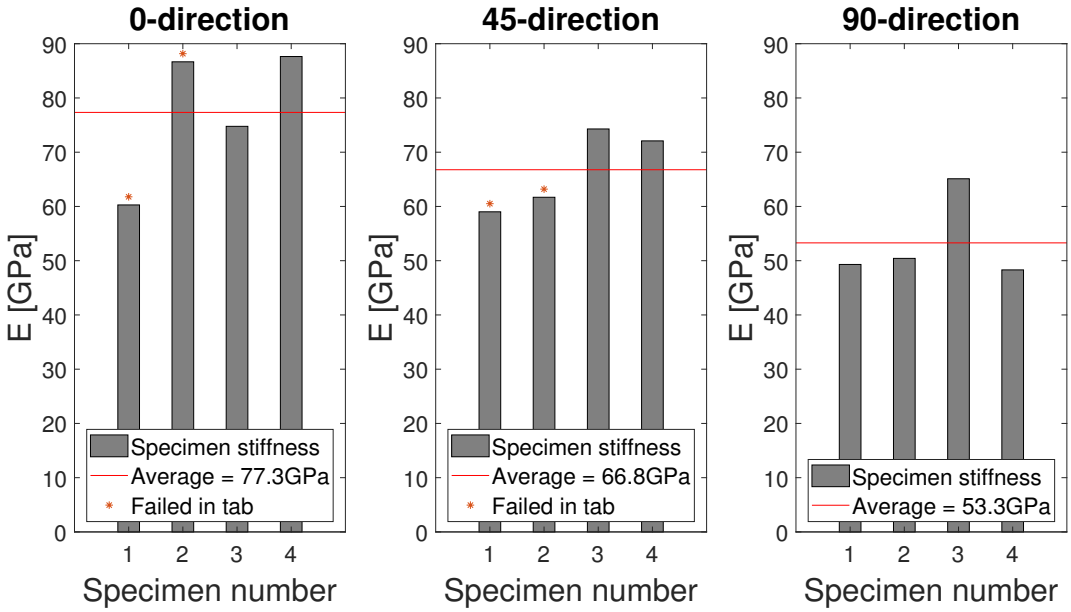

Figure 4.11: Measured stiffness in plate no.2 for three directions. Specimens which failed in tab are marked with an asterisk.

Tensile strength also varies, see Figure 4.12 and Figure 4.13. Average strengths for plate no.1 and plate no.2 are measured to 330.1 MPa and 343.8 MPa. However, during testing 7 out of 24 specimens

failed in the tab. These were hence all premature failures, and if the strengths for these are neglected new adjusted average tensile strengths for plate no.1 and no.2 are 368.6 MPa and 423.9 MPa. Some specimens reach tensile strengths close to 500 MPa.

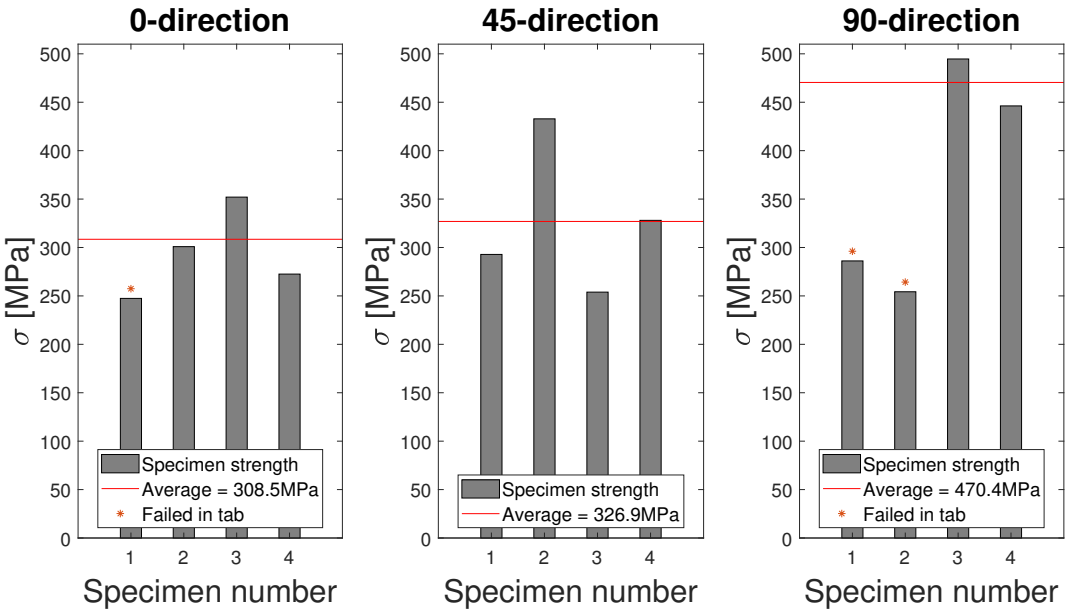

Figure 4.12: Measured tensile strength in plate no.1 for three directions. Specimens which failed in the tab are marked with an asterisk.

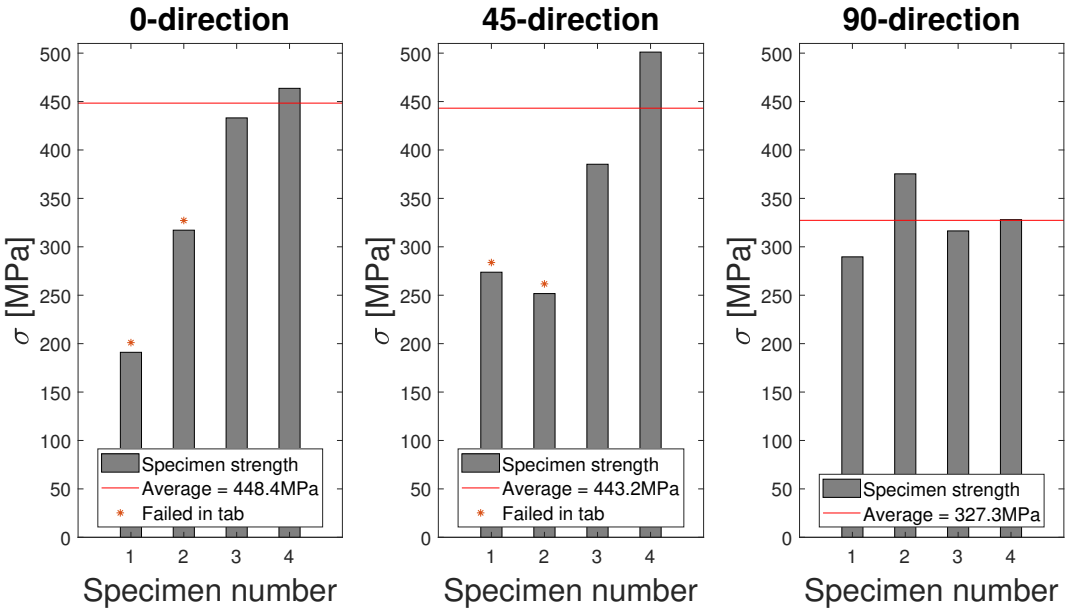

Figure 4.13: Measured tensile strength in plate no.2 for three directions. Specimens which failed in the tab are marked with an asterisk.

The strain to failure, presented in Figure 4.14 and Figure 4.15, is on average 0.54 % for both plates. Yet, if the specimens that broke in the tab are discarded, plate no.1 displays an average strain to failure at 0.57 % and plate no.2 at 0.61 %. The maximum strain to failure recorded is 0.75 %. Furthermore, the strain over the specimen surface, just before failure, varies to a high degree as can be seen in Figure 4.16. Large regions of high strain mingled with large regions of low strain indicate high material heterogeneity.

Poisson's ratio was calculated from the strain in longitudinal and transverse direction measured with DIC. Figure 4.17 show the Poisson's ratio for each specimen. The values are scattered with an average ratio at 0.39 %.

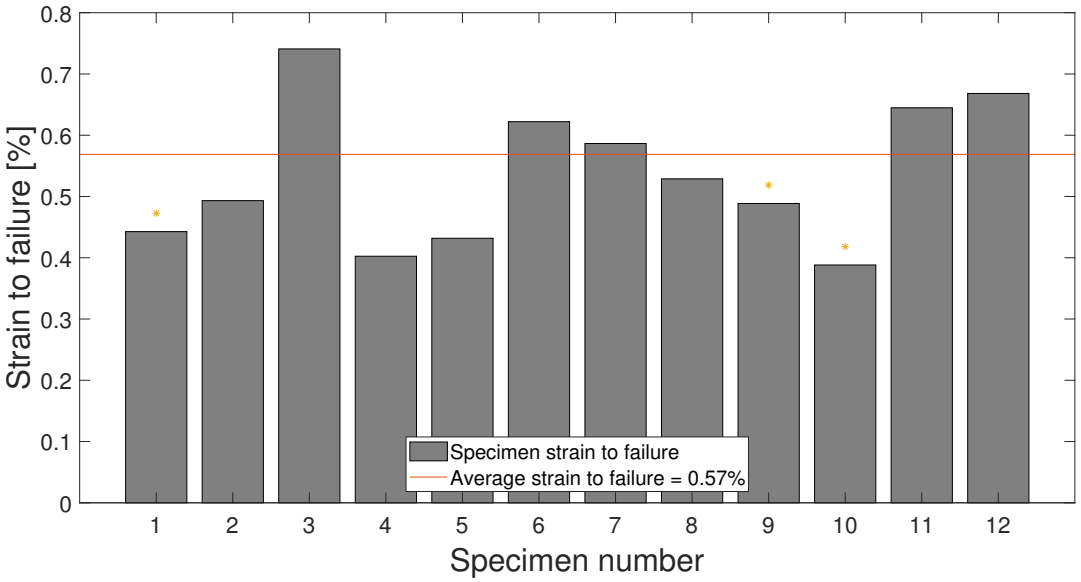

Figure 4.14: Measured strain to failure in specimens from plate no.1

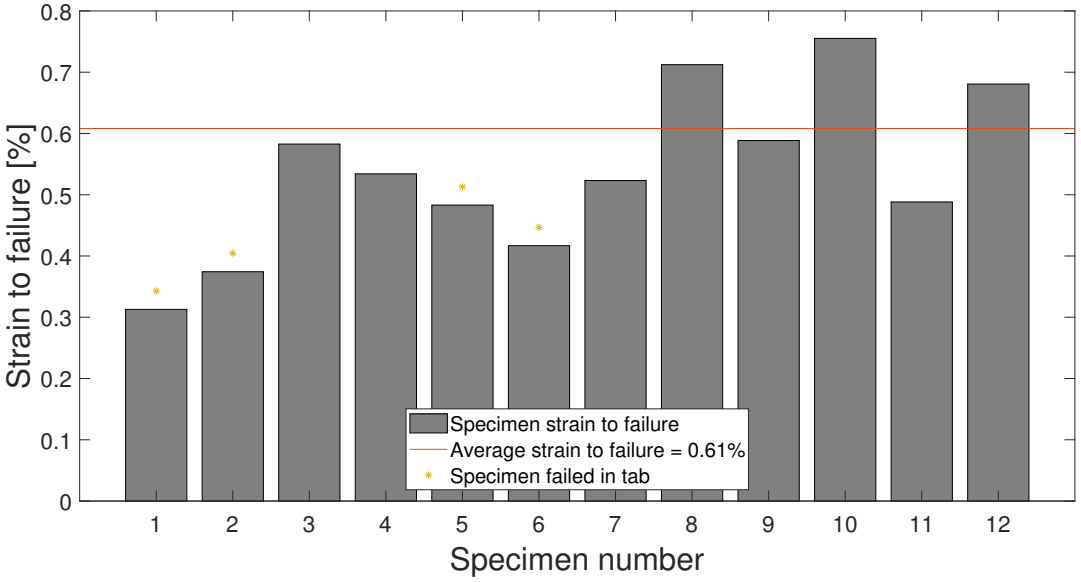

Figure 4.15: Measured strain to failure in specimens from plate no.2

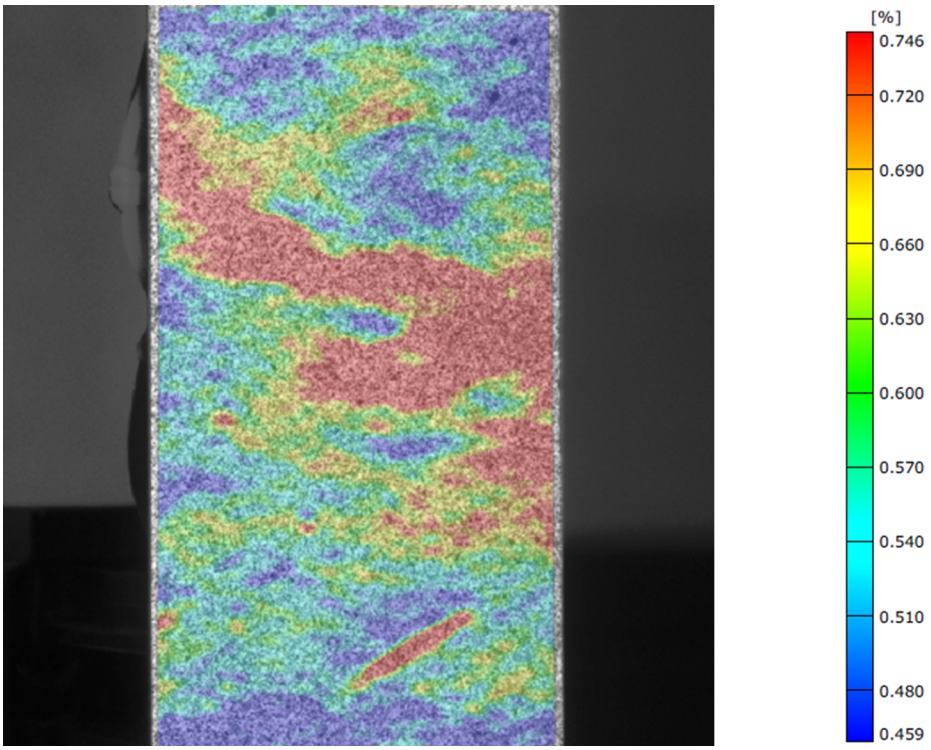

Figure 4.16: A strain field of a specimen surface just before failure. The measured strain is heterogeneous. The red regions indicate high strain and the blue regions indicate low strain.

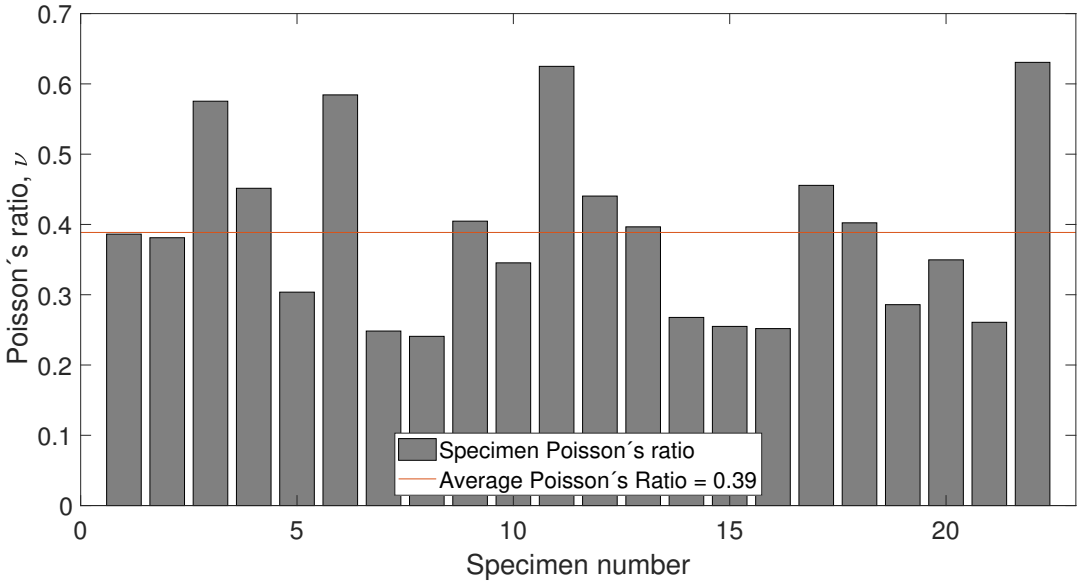

Figure 4.17: Measured Poisson's ratio for all specimens.

4.6 Fractography

Two modes of fracture are present in the UTHMT composite material tested in tension: delamination-dominated failure through tape pullout and fibre-dominated failure through longitudinal fibre failure. Figure 4.18 shows a tape surface revealed by tape pullout. The greatest magnification of the stereo microscope captures the fibres exposed by two tapes shearing relative one another. The presence of raised platelets, referred to as cusps, in the fibre tracks is evidence of mode II fracture [11] and Figure 4.19 therefore shows multiple cusps and debris stemming from tape pullout. Fibre tension failure is seen in Figure 4.20 where the presence of radial markings on the fibre ends indicate fibres breaking during tensile load [12]. The presence of these two fracture modes correlates strongly with predictions reported by Persson [13]. His material model for composites based on tapes with uniform orientation distribution predicts tape pullout for tapes oriented 20° to 90° off-axis of the load direction. The same model predicts fibre failure for tapes 0° to 20° off-axis.

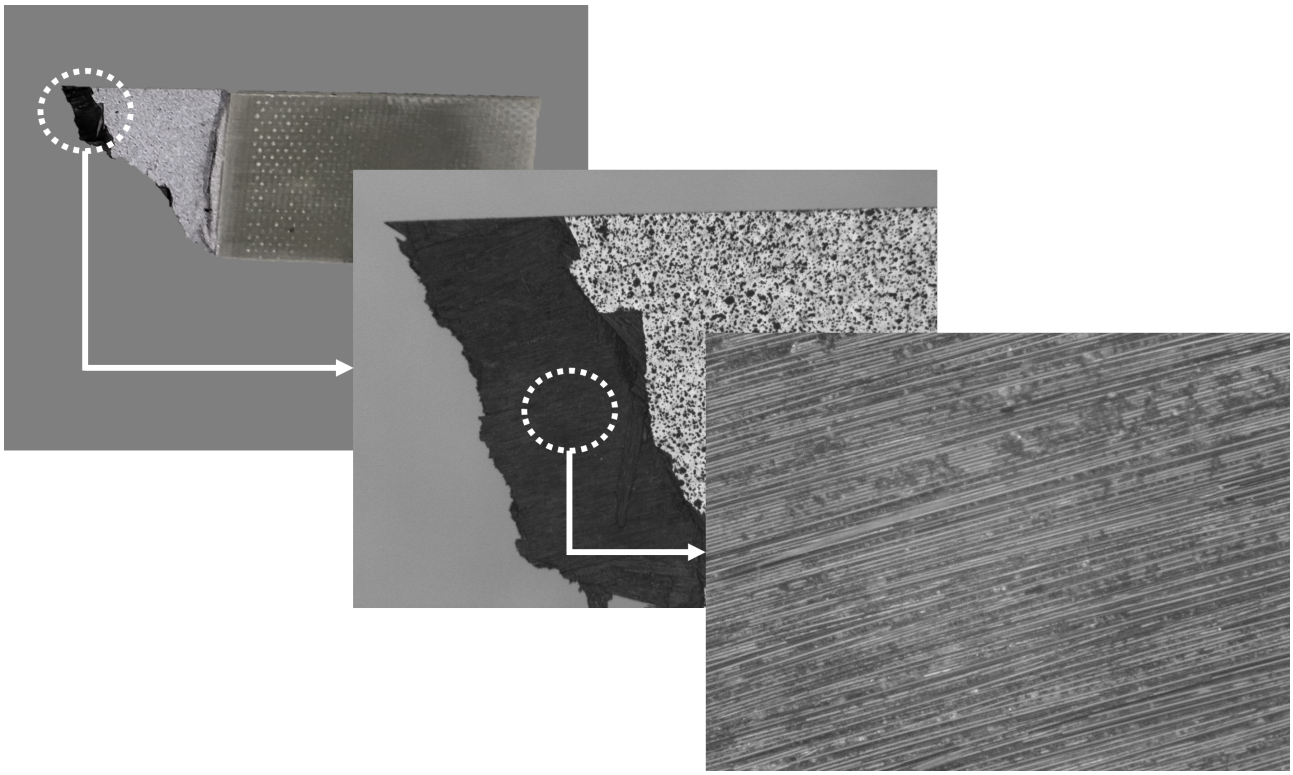

Figure 4.18: Three magnifications of the same fracture surface. The surface has been revealed through tape pullout.

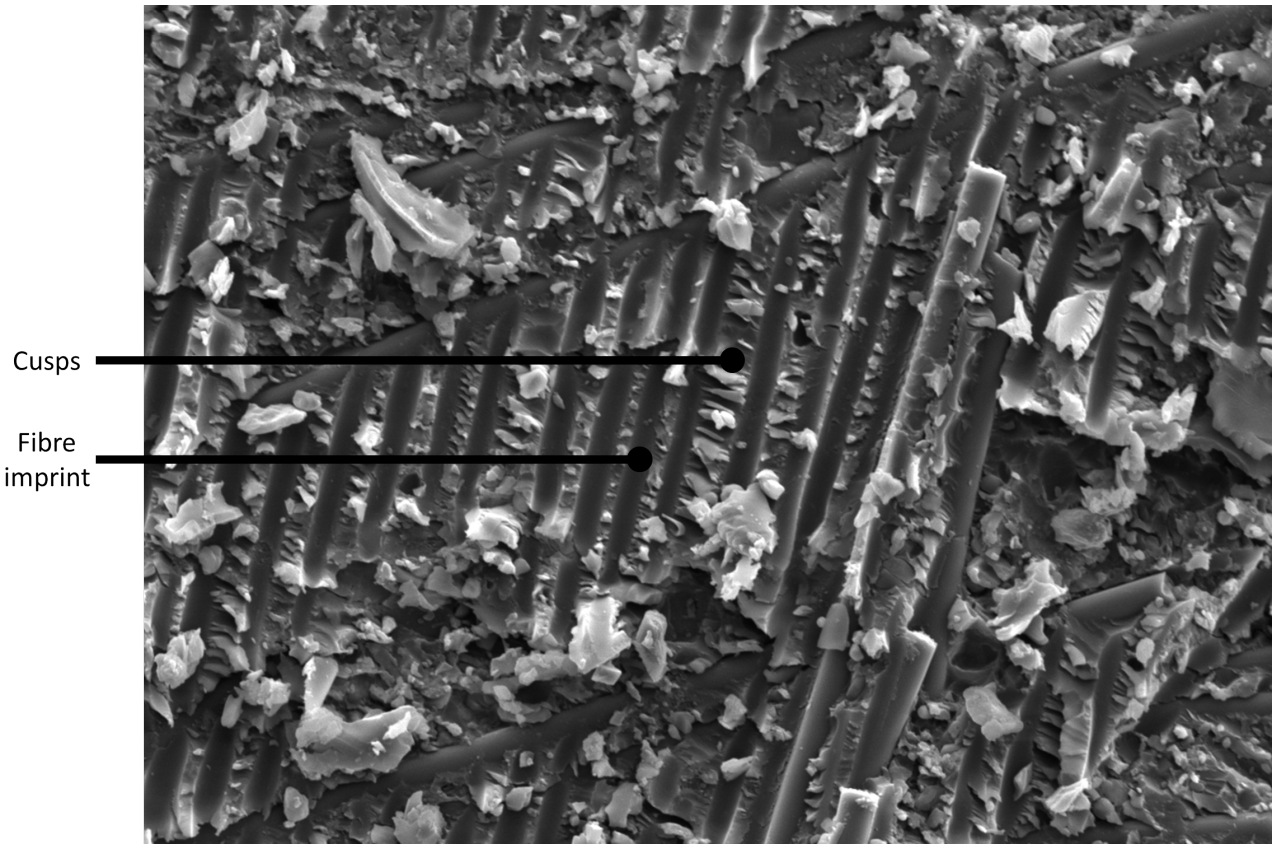

Figure 4.19: SEM-image of a fracture surface generated by tape pullout. Between the fibre imprints the cusps stemming from mode II fracture can be seen.

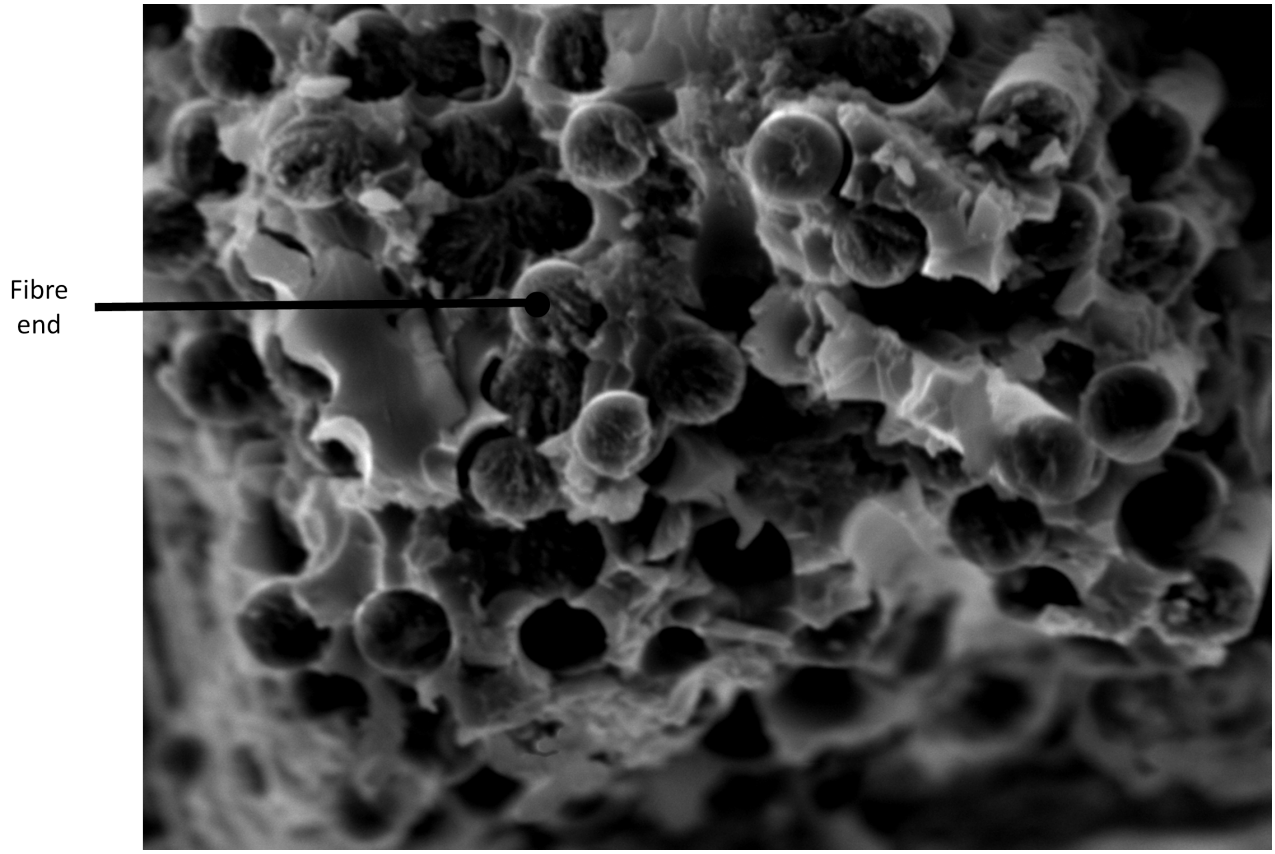

Figure 4.20: SEM-image of failed fibres in the load direction. At the fibre ends radial markings are present, which indicate fibre fracture through tension.

5

Discussion

In this chapter are the methodology, results and future improvements discussed. Possible sources of error in manufacturing and characterisation are explored together with how the errors have influenced the results. The results are compared with previous works. The chapter ends with suggested improvements and the possible consequences of implementing them.

5.1 Mechanical response

The tensile test results show promising stiffness properties for the material. The average stiffness is 50 GPa higher than what Darvell produced [6] and 15 GPa higher than what what Takahashi and colleges produced [5]. However, the scattering of stiffness values is noticeable. Complete in-plane isotropy has not been achieved and the reason is probably that the orientation distribution of tapes is not entirely uniform. In plate no.2 there is a quite clear trend that the stiffness increases as the orientation shifts towards the 0°-direction, see Figure 4.11. Presumably there are more fibres in the 0°-direction, but the trend can also depend on localised properties. In Figure 3.4 it can be seen where the specimens were cut. All specimens for one specific direction are extracted from the same region of the plate for sake of convenience. This can lead to all specimens of that direction attracting the same defect, which then affects the results. The most plausible type of defect is thickness variations as can be seen in Figure 4.4, but pockets of resin in Figure 4.8 and 4.9 or waviness in Figure 4.7 are also defects which can influence the mechanical properties. Nonetheless, the most likely reason is non-uniform orientation distribution.

The values for tensile strength are also encouraging with some exceptionally high measured strengths of parity with Takahashi [5], meaning that the UTHMT composite material is stiffer without losing strength. Though, the strength values are scattered. The variation among the specimens is probably due to uneven thickness. Since an average thickness for each specimen is used for calculation of stresses the experienced stress of the thinnest region will be underestimated. The heterogeneous strain field in Figure 4.16 indicates that the stresses in the material have varied extensively. Furthermore, the specimens which failed in the tab region can prove to have had very high strength, but since the tab influenced the test these high strengths were never recorded. Since stiffness and strength varies, the strain to failure also varies owing to the non-uniform orientation distribution and uneven thickness.

Like the other mechanical properties, Poisson's ratio greatly differ between specimens. However, an additional reason for this is probably the measuring method. DIC only measures strain on the surface of the specimen and therefore the tapes on the surface heavily influences the measurement. With the tapes being almost the size of the observed area on the surface of the specimen, tapes of different orientation will lead to very different values of Poisson's ratio.

5.2 Characterisation

Firstly, differential scanning calorimetry is a basic experiment, yet, it relies on accurate references. For the DSC experiment performed the validity of the reference materials have not been confirmed. Potentially, the cured reference material may not be fully cured. However, everything indicates that the reference was hundred percent cured.

It should be noted that samples for both matrix digestion and cross-section analysis were taken from very local regions. This means that the results are representative of these regions, but there is a risk that other regions of the material do not display the same properties. Convenience and a limited amount of material were the grounds for this. Additionally, regarding the cross-section analysis, note that the width and the length of a tape by far exceeds the dimensions of the examined area in the compound microscope. To produce a complete cross-section of one tape at least 30 images are needed to be stitched together. Due to this and the challenge of determining the orientation of a tape in the middle of the material, the characteristics of a complete tape has not been examined.

As stated in Section 3.4 no standard was used for the tensile test since the specimens were too thin. With a thinner cross-section the influence of thickness variation becomes greater. It can then be argued that a thicker plate should have been produced, but the reason behind a thin material was the demand for thin applications by industry. It was deemed more important to investigate the potential of the concept for very small thicknesses than to perform a perfect tensile test. Further, the application of tabs was done relatively quick. Preferably the post cure takes two weeks in room temperature. Instead the curing was done at 70 °C for 24 h. The material is supposed to withstand a temperature of 70 °C since the glass transition temperature for the cured matrix is 120 °C, but there is a risk that it can have affected the specimens.

With limited access to SEM not enough time for fractography was at the disposal to identify fracture initiation points. The initiation point is of great interest to understand the failure mechanisms. This thesis work presents two distinct fracture features in a UTHMT composite material, but no conclusion on which of the two fracture modes happens first can be drawn.

5.3 Manufacturing

Initially a lot of time of the thesis work went into manufacturing of the UTHMT composite material. The resources were spent on mitigating problems of tape wrinkling, resin smearing of the chopper, proper fibre wetting and many other small practical adjustments. These challenges were eventually solved to a satisfying degree, however, problems with uniform tape orientation distribution and uniform thickness still need improvement as is evident by the tensile test results. These two parts of manufacturing are difficult to control, but it is more a question of good engineering than if it is possible to do or not. The challenge comes in the contradicting nature of having a random variable deeply connected with a fixed variable. The orientation of the tapes is supposed to be random but the falling position, and in extension the thickness, is supposed to be everything but random. The method of falling tapes can be challenged in its entirety, however, manual hand lay-up or wet-type paper making process are enormously more time consuming. Therefore the lay-up method used by this thesis work is still interesting. It can be stated with certainty that the mechanical results will show much less scattering if the lay-up is further improved.

Forming can also be revised. It is problematic that the pressure applied during curing was manually controlled without any actual measurement of the pressure. Even though the material is cured, owing to the uncertainty regarding the pressure, it cannot be concluded that an optimal liquid pressure was achieved. In addition, the vacuum used was not perfect. The tacky tape around the cavity did seal well enough, but with higher vacuum even less pores would have remained in the material. Finally,

the resin content was high in the material and this definitely affects the mechanical properties. The tape finally used had first 38 % weight fraction resin sprayed on one side. To have resin on both sides, additional resin was sprayed so the final resin content was 45.5 % correlating to a fibre volume fraction in the tape of 43 %.

5.4 Suggested improvements

With the aim to produce an even stiffer, stronger and in-plane isotropic material there are several things that can be improved. Firstly, a more even plate thickness is crucial. The thickness is controlled by the number of tapes stacked on each other, which in turn is controlled by the number of falling tapes and the number of possible landing position. By limiting the number of landing positions the influence of uneven distribution decreases. A suggested improvement is therefore to shrink the cross-section of the falling channel in one direction and use a rectangular cross-section instead in conjunction with a moving substrate in the form of a conveyor belt. The landing position will be limited to a smaller strip with a length of the conveyor belts width. Of course the width of the slimmer falling channel will have to be larger than a tape length. This setup can be connected to a lamination machine to further automate the process. The new challenges arising from this approach will be the effect on tape orientation by the walls of the tighter falling channel and the moving conveyor belt. With a non-square shape the channel walls will potentially induce a favoured tape direction. On the other hand, a moving substrate will also influence the tapes to orient in a direction parallel to the movement. Since the directing by the channel and the conveyor belt are perpendicular, the shape of the channel and velocity of the belt can be optimised to allow for uniform tape orientation distribution. Also multiple start positions of falling tapes would even out the distribution, so instead of only one chopper, several choppers can be used. This can also increase the production speed.

As the number of tapes too influence the thickness, this can be optimised by changing the dimensions of the chopped tapes. With shorter tapes the number of tapes will increase and with more tapes the presence of a "misplaced" tape will not be as impactful. However, a consequence of more tapes is more tape ends. As the cross-section images in Section 4.4 suggest, tape ends give rise to resin pockets and waviness. The resin pockets are weakening the material and wavy fibres are not preferable for compressive load bearing. These aspects have to be considered when optimising tape dimensions, but an advantage of shorter tapes are potentially higher processability of complex geometry. In realised applications the material will not only be shaped as a plate and by using shorter tapes the amount of curved fibres will be reduced.

So far improvements for first manufacturing method and then tape dimensions have been discussed, but if focus shifts to an even smaller scale, there are more potential areas of improvement. The constituents of the tape can be further developed. Starting with the reinforcement, the fibres can be upgraded to stiffer fibres, which will boost the composite stiffness. Yet, when fibre stiffness increases the strain to failure tends to decrease. How lower strain to failure will affect a UTHMT composite is still to be investigated, but it is reasonable to assume that at a point the composite strength will be affected by too low strain to failure. Nonetheless, there is possibly a great range of ultra-stiff fibres which can be utilised in a UTHMT composite material. This would open up a completely new field for brittle but stiff fibres not used today. Moreover, an increased fibre volume fraction will enhance the mechanical properties of the material. Therefore a lowered amount of is resin a very important aspect to develop. Tapes with resin applied on both sides circumvent the need of resin permeating through the tape and so the resin content can be lowered to increase stiffness and strength.

5.5 Future work

Further investigations into UTHMT composite materials comprehend a plethora of areas: tape distribution, automation of production, effects of tape dimensions, effects of higher fibre volume fractions close to 60 %, influence of tape ends, resin flow in thin materials based on ultra-thin tapes, effect of even stiffer tapes, compression tests, bending tests and so on. However, the most interesting aspect to study in more depth is the initiation point of fracture. Does the fracture always start in tapes with a specific angle to the load direction? How does the initiation point change when the the material constituents change? These questions can be attempted to be answered by future work, but it is certain that further research will lead to more questions and more exciting challenges.

6

Conclusion

A composite material consisting of randomly oriented CFRP tapes has been manufactured and characterised. The manufacturing included production of preforms of tapes with resin sprayed on both sides, cut to lengths of 40 mm and distributed through a falling channel onto a step-wise rotating substrate. The preforms were cured to stiff plates in a heat press and then characterised and mechanically tested. Complete isotropy was almost achieved and average stiffness and strength reached 64.2 GPa and 395.25 MPa. The fracture modes of the material was determined to be tape pullout and fibre tension failure. This Master's thesis work shows that there is great potential in a material of uniformly oriented ultra-thin high modulus CFRP tapes.

Bibliography

[1] A. P. Jackson, J. F. V. Vincent, R. M. Turner. "The mechanical design of nacre", *Proc. Royal Society B: Biol. Sci.*, vol. 234, no. 1277, 1988, pp. 415-440.

[2] Y. Wan, J. Takahashi. "Tensile properties and aspect ratio simulation of transversely isotropic discontinuous carbon fiber reinforced thermoplastics", *Composites Science and Technology*, vol. 137, 2016, pp. 167-176.

[3] S. Pimenta, P. Robinson. "An analytical shear-lag model for composites with 'brick-and-mortar' architecture considering non-linear matrix response and failure", *Comp. Sci. Technol.*, vol. 104, 2014, pp. 111–124.

[4] Y. Li, S. Pimenta, J. Singgih, S. Nothdurfter, K. Schuffenhauer. "Experimental investigation of randomly-oriented tow-based discontinuous composites and their equivalent laminates" *Composites Part A: Applied Science and Manufacturing*, vol. 102, 2017, pp. 64-75.

[5] Y. Wan, I. Straumit, J. Takahashi, S. V. Lomov. "Micro-CT analysis of the orientation unevenness in randomly chopped strand composites in relation to the strand length" *Composite Structures*, vol. 206, 2018, pp. 865-875.

[6] M. Darvell. "Randomized CFRTP tape piece laminates in structural automotive applications", Master's thesis, Department of Lightweight Structures at Aeronautical and Vehicle, KTH Royal Institute of Technology, 2015.

[7] R.A. Fava. "Differential scanning calorimetry of epoxy resins" *Polymer*, vol. 9, 1968, pp. 137-151.

[8] *Standard Test Methods for Constituent Content of Composite Materials*, ASTM D3171, ASTM International, West Conshohocken, PA, 2015.

[9] *Standard Test Method for Tensile Properties of Polymer Matrix Composite Materials*, ASTM D3039 / D3039M, ASTM International, West Conshohocken, PA, 2017.

[10] E. S. Greenhalgh. "Introduction to failure analysis and fractography of polymer composites" *Failure Analysis and Fractography of Polymer Composites*, 1st ed. Cambridge, UK: Woodhead, 2009, ch. 2, pp. 23-106.

[11] E. S. Greenhalgh. "Delamination-dominated failures in polymer composites" *Failure Analysis and Fractography of Polymer Composites*, 1st ed. Cambridge, UK: Woodhead, 2009, ch. 4, pp. 164-237.

[12] E. S. Greenhalgh. "Fibre-dominated failures of polymer composites" *Failure Analysis and Fractography of Polymer Composites*, 1st ed. Cambridge, UK: Woodhead, 2009, ch. 4, pp. 107-163.

[13] M. Persson. "Mechanical analysis methods for ultra-stiff CFRP from thin tapes", unpublished.